

# Improvements in Monte Carlo simulation of large electron fields

Bruce A Faddegon<sup>1</sup>, Joseph Perl<sup>2</sup> and Makoto Asai<sup>2</sup>

<sup>1</sup>University of California San Francisco Comprehensive Cancer Center  
1600 Divisadero Street  
San Francisco, CA, 94115-1708, USA  
Email: bfaddegon@radonc.ucsf.edu

<sup>2</sup>Stanford Linear Accelerator Center  
2575 Sand Hill Road  
Menlo Park, CA 94025, USA

Keywords: Monte Carlo, electrons, treatment head simulation, beam modeling

**Abstract.** Two Monte Carlo systems, EGSnrc and Geant4, were used to calculate dose distributions in large electron fields used in radiotherapy. Source and geometry parameters were adjusted to match calculated results with measurement. Both codes were capable of accurately reproducing the measured dose distributions of the 6 electron beams available on the accelerator. Depth penetration was matched to 0.1 cm. Depth dose curves generally agreed to 2% in the build-up region, although there is an additional 2-3% experimental uncertainty in this region. Dose profiles matched to 2% at the depth of maximum dose in the central region of the beam, out to the point of the profile where the dose begins to fall rapidly. A 3%/3mm match was obtained outside the central region except for the 6 MeV beam, where dose differences reached 5%. The discrepancy observed in the bremsstrahlung tail in published results that used EGS4 is no longer evident. The different systems required different source energies, incident beam angles, thicknesses of the exit window and primary foils, and distance between the primary and secondary foil. These results underscore the requirement for an experimental benchmark of electron scatter for beam energies and foils relevant to radiotherapy.

## 1. Introduction

Monte Carlo simulation is a technique that provides both accurate and detailed calculation of particle fluence from the treatment head of a radiotherapy linear accelerator. The method was reviewed by Ma and Jiang (1999) for electron beams and by Verhaegen and Seuntjens (2003) for x-ray beams.

Faddegon et al (2005) used Monte Carlo simulation of the treatment head to calculate dose distributions in water for the largest electron field available on commercial linear accelerators used in radiotherapy, the 40x40 cm field with no applicator. This large-field geometry produced a clean beam with low contamination from collimator scatter. The passage of the electron source particles and the resulting electromagnetic cascade were simulated from the exit window through the scattering foils, collimators and monitor chamber, out past the adjustable collimators (jaws and MLC) and into a water phantom (Figure 1).

The dose distributions were sensitive to details of both the source, at the exit window of the accelerator, and to the geometry of the treatment head (Schreiber and Faddegon, 2005). This included significant sensitivity to asymmetry in the source and geometry, including non-normal incidence of the source particles at the exit window and off-axis shifts of the center of the secondary scattering foil and monitor chamber. Calculated and measured dose distributions were generally in excellent agreement, although there was a significant discrepancy in the dose in the bremsstrahlung region beyond the practical range of the primary electrons, relative to the maximum dose on the central axis.

The simulation was done using the BEAM user code with the EGS4 Monte Carlo system (Rogers et al, 1995). The EGSnrc system, a revision of EGS4, has a variety of improvements to electron transport (Kawrakow, 2000). These improvements make it relevant to revisit this problem.

The large field measurements proved useful for uncovering problems with radiation transport in EGS4. Geant4 is an all particle code with applications covering a variety of fields. A primary application in medical physics is particle therapy. Recent work has uncovered some problems in the use of Geant4 for simulation in external beam radiotherapy (Poon and Verhaegen, 2005). It is relevant to establish the capability of Geant4 in matching the measured dose distributions in large electron fields.

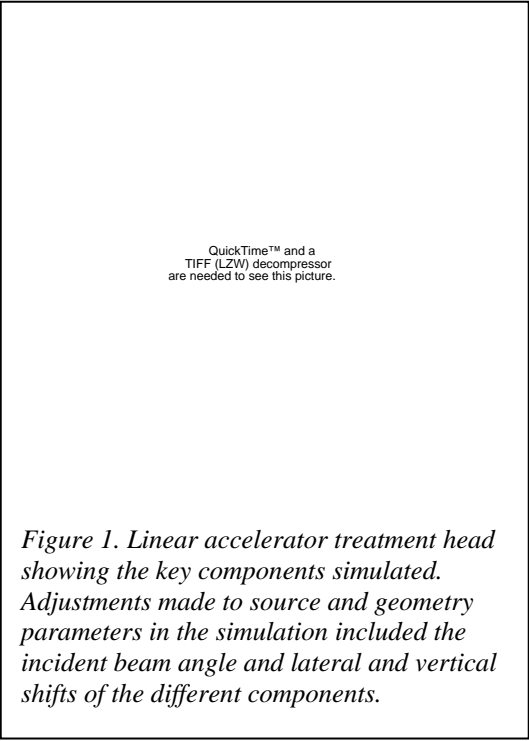
In this work, published measurements in large electron fields are compared to calculations using both EGSnrc and Geant4. Results show whether these codes provide for a better match than in the earlier publication and whether this match requires different source and geometry parameters. Implications for the accuracy of the calculated dose and fluence are discussed.

## 2. Materials and Method

### 2.1 Measurement

The measurements reported here are the same measurements used in the previous study (Faddegon et al, 2005). Details of the experimental method are given in that publication. Measurements were made on a Siemens Primus linear accelerator. The field size was set at the maximum, 40x40 cm, with no applicator. Measurements were done in water at 100 cm SSD. The central axis depth dose curve was measured for each beam along with a set of orthogonal profiles taken at the depth of maximum dose,  $d_{max}$ , and at a depth beyond the practical range,  $R_{p+}$ , where dose is from bremsstrahlung produced in the treatment head and water.

Depth dose curves were measured with both a diode (Scanditronix EFD "blue" diode) and a parallel plate ion chamber (PTW-Freiberg Roos N-34001). In the current study, the parallel-plate measurements were corrected with published stopping-power ratios for mono-energetic beams (Khan et al, 1991). This permitted direct comparison of the depth dose curves measured with the



QuickTime™ and a  
TIFF (LZW) decompressor  
are needed to see this picture.

*Figure 1. Linear accelerator treatment head showing the key components simulated. Adjustments made to source and geometry parameters in the simulation included the incident beam angle and lateral and vertical shifts of the different components.*

diode and parallel-plate chamber with the results of the Monte Carlo simulation on the same graph.

Profiles at  $d_{\max}$  were measured with the diode, profiles in the bremsstrahlung tail with a thimble ion chamber (PTW CC13). The AAPM dosimetry protocol (Almond et al 1999) was used to measure the dose from x-rays at  $R_{p+}$ , using a Farmer type chamber, and the dose from electrons at  $d_{\max}$ , using a parallel-plate chamber. Measured profiles in the bremsstrahlung region were normalized to the ratio of these doses,  $D_x/D_e$ , then multiplied by a factor,  $k_V$ , which depended on the beam energy, to correct to the average dose over the 0.8 cm depth of the calculated profiles at  $d_{\max}$ .

## 2.2 Monte Carlo Simulation

The simulations were done using the methodology employed in the previous study. A parallel beam of electrons with energy distribution calculated with the Parmela code was incident at a non-normal beam angle, in a radially symmetric, Gaussian-shaped focal spot. The beam passed through the water-cooled exit window of the treatment head, then through a set of two scattering foils, the second a shaped foil attached to the monitor chamber. Jaws and MLC were set to the maximum field size setting, corresponding to a field of 40x40 cm at the isocenter of the machine, 100 cm from the source. There was no electron applicator.

Dose distributions were calculated in a 60x60x15 cm water phantom, with the beam directed in the z-direction. The 60x60 cm square surface was centered on the central axis of collimator rotation. The phantom was positioned with the water surface at the machine isocenter. Energy deposited in the phantom was accumulated in 0.3x0.3x0.2 cm voxels. To improve statistics, depth dose distributions were rebinned prior to plotting to 1.8x1.8x0.2 cm voxels for depth dose curves, with the highest resolution of 0.2 cm preserved in the depth direction. Profiles were rebinned, depending on the orientation of the scan (inplane or crossplane), to either 0.3x1.8x0.8 cm or 1.8x0.3x0.8 cm at  $d_{\max}$ , and to either 0.3x3.6x1.6 cm or 3.6x0.3x1.6 cm at  $R_{p+}$ . There were 50,000,000 source particles for each beam simulated. The statistical precision of the calculation, one standard deviation, was 0.4% for the depth dose curves near  $d_{\max}$  and 0.5% for the profiles at  $d_{\max}$  at points in the treatment field (well inside the penumbra). The precision was 1-3% for the profiles at  $R_{p+}$  at points near the central axis. The higher precision was obtained at higher energy, as more bremsstrahlung is present in the beam at these energies.

Parameter adjustment was done iteratively until a good match with measurement was achieved or the match was deemed to approach the best possible for the particular simulation code used and the statistics in the calculated result. A good match was defined as 1 mm or better for depth penetration, in the fall-off region of the depth dose curve, from 20% to 80% of the maximum dose, and as 2%/2mm for the  $d_{\max}$  profiles. That is, with the dose normalized to 100% at  $d_{\max}$ , either the dose difference is within 2% or the distance between the depth dose curves is within 2 mm, or both. A 5% match was sought to the dose ratio  $D_x/D_e$ , and to the profile measured just beyond the practical range.

## 2.3 EGSnrc

The treatment head was simulated with the EGS user code BEAM of Rogers et al (1995), version BEAMnrcMP 20007, with beamnrc.mortran version 1.77 of October 4, 2006. The EGS user code MCRTTP version 2.0 of May 31, 2007 was used to simulate the water phantom. Both user codes utilized EGSnrc version V4-42-2-5 of February 13, 2007. Transport parameters included electron lower energy cut-offs ECUT and AE of 0.7 MeV, and photon lower energy cut-offs PCUT and AP of 1 keV. Other parameters included a maximum step size SMAX of 5 cm, ESTEPE of 0.25,

XIMAX of 0.5, skin depth for BCA defaulted, spin effect on, bremsstrahlung angular sampling and pair angular sampling both “Simple,” and bremsstrahlung cross section Bethe-Heitler. Bound Compton scattering, Rayleigh scattering, atomic relaxations, and photoelectron angular sampling were all turned off.

The starting point for the EGSnrc simulation was the published result for EGS4 (Faddegon et al, 2005). The energy distribution of the source was the same as in that publication. The mean energy was adjusted by shifting the spectrum to match the measured depth penetration in the calculated dose distribution. Further adjustments included both cross-plane and in-plane beam angle, thickness of materials that scatter the beam and produce bremsstrahlung, and lateral and vertical shifts of the different components that scatter and collimate the beam, as depicted in Figure 1.

#### 2.4 Geant4

The Geant4 Simulation Toolkit, version 8.2.p01 of February 23, 2007, was used to simulate the treatment head and water phantom. All material definitions were taken from the NIST material definitions built into Geant4, with the exception of the stainless steel and the beam vacuum, which were defined as compositions of appropriate NIST elements. The water phantom was implemented as 200x200x75 voxels each of size 3x3x2 mm.

Simulation was done for two different sets of radiation transport parameters. The list of processes to simulate (“physics list” in Geant4 terminology) in the first set, the “standard” physics list, was taken from one of the standard examples distributed with Geant4, example TestEM7 (physics list named “PhysListEMStandard”). A low value of 0.001 mm was chosen for the Range Cut parameter for the first set of Geant4 simulations. The second set of simulations used the “low energy” physics list (“PhysListEmLivermore,” taken from the same published Geant4 example TestEM7). A change in range cut from 0.001 mm to 1 mm had no more than a 2%/2mm affect on the calculated dose distributions for either physics list. There was no noticeable effect on the bremsstrahlung dose outside of statistics.

The starting point for the Geant4 simulations using the standard physics list was the final values of the EGSnrc simulations. Further adjustments were done until a reasonable match to the measured data was found. This gave the starting point for the Geant4 simulations using the low energy physics list.

### 3. Results and Discussion

#### 3.1 Depth dose curves

Measured depth dose curves are shown in Figure 2. Both diode and parallel-plate measurements are shown. The sharp drop in the dose in the bremsstrahlung tail at 12 MeV is due to a change to a thicker primary scattering foil at 15 MeV. The highest three energies share the same foil.

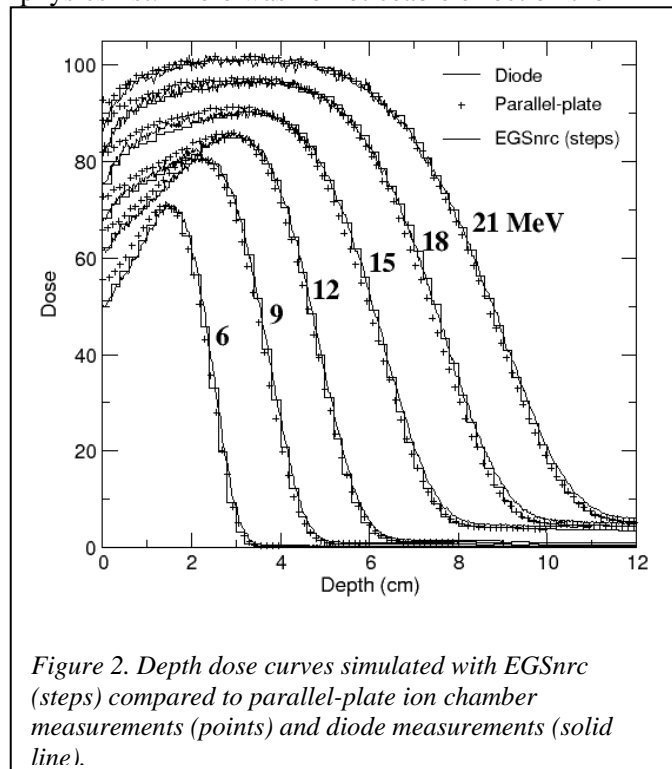


Figure 2. Depth dose curves simulated with EGSnrc (steps) compared to parallel-plate ion chamber measurements (points) and diode measurements (solid line).

As with EGS4, the EGSnrc results (Figure 2) compare more favourably with the diode measurements from the surface to the depth of 80% of the maximum dose and with the parallel-plate measurements beyond that depth. These specific measurements agree with the calculated results to 2%/1mm or better at all energies. There are discrepancies with the parallel-plate measurements near the surface as large as 4% for some of the beam energies.

Depth dose curves calculated with Geant4 using the 2 different physics lists are shown in Figure 3. Unlike the EGSnrc results, the Geant4 results compare more favourably with the parallel-plate measurements than the diode measurements. The energy in the simulation was chosen to match the penetration depth measured with the parallel-plate chamber. The calculated depth dose curves are within 2%/1mm of the parallel-plate measurements at all depths with one exception: The 6 MeV beam calculated using the low energy physics list. In this case there is a higher surface dose and a shallower penetration than measured or calculated in simulations done with the standard physics list or with EGSnrc. A statistically independent run was repeated for the 6 MeV beam with the same result. Range cuts of 0.001 mm and 0.1 mm resulted in the same depth dose curve within 2%. This may point to a problem with the simulation for the lowest beam energy when using the low energy physics list.

Consider the difference in dose in the build-up region between the measurements with diode and parallel-plate chamber. The stopping power ratio (SPR) applied to the ion chamber measurements is shown in Figure 4. Monte Carlo simulation using a realistic beam provides a more accurate SPR (Ding et al, 1995). Water-to-air and water-to-silicon SPR's calculated with MCRTTP for the electron beams simulated in this study are also plotted in Figure 4. The two sets of curves are shifted relative to each other since they correspond to slightly different incident beam energies. This is because the SPR

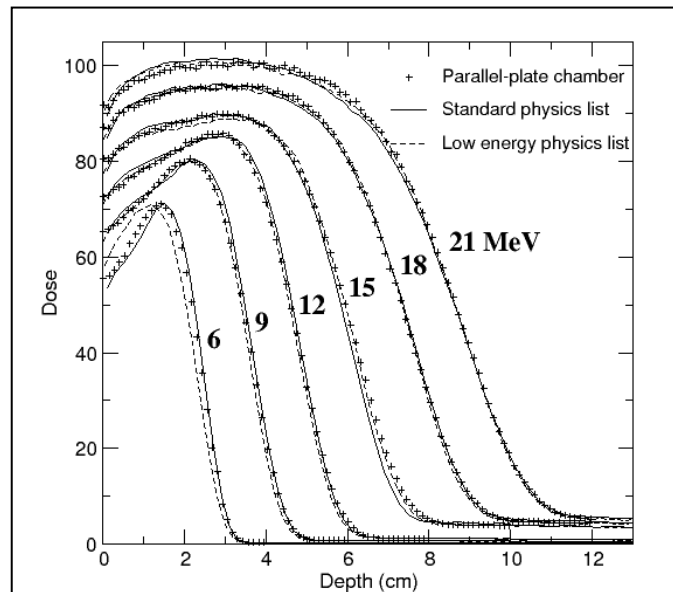


Figure 3. Depth dose curves calculated with Geant4 with the standard physics list with 0.001 mm range cut (solid line) and low energy physics list with 0.1 mm range cut (dashed line), compared to the parallel-plate measurements from Figure 2 (points).

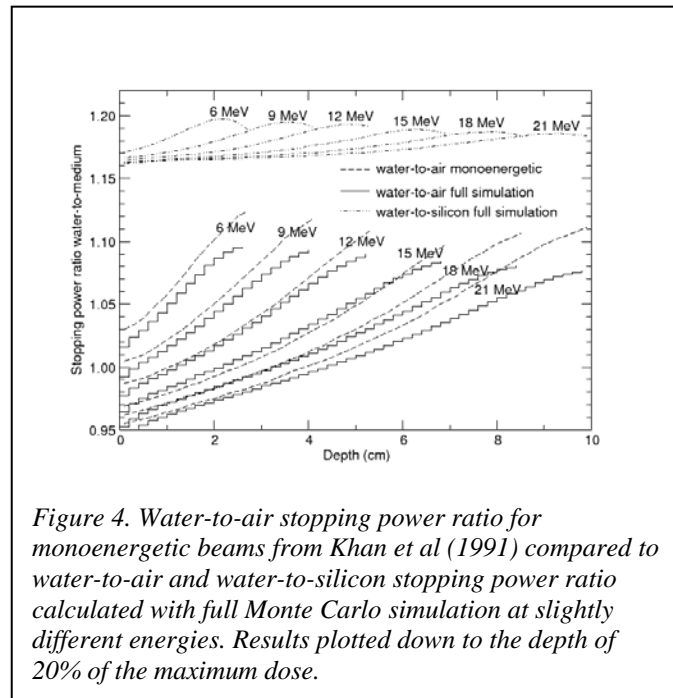


Figure 4. Water-to-air stopping power ratio for monoenergetic beams from Khan et al (1991) compared to water-to-air and water-to-silicon stopping power ratio calculated with full Monte Carlo simulation at slightly different energies. Results plotted down to the depth of 20% of the maximum dose.

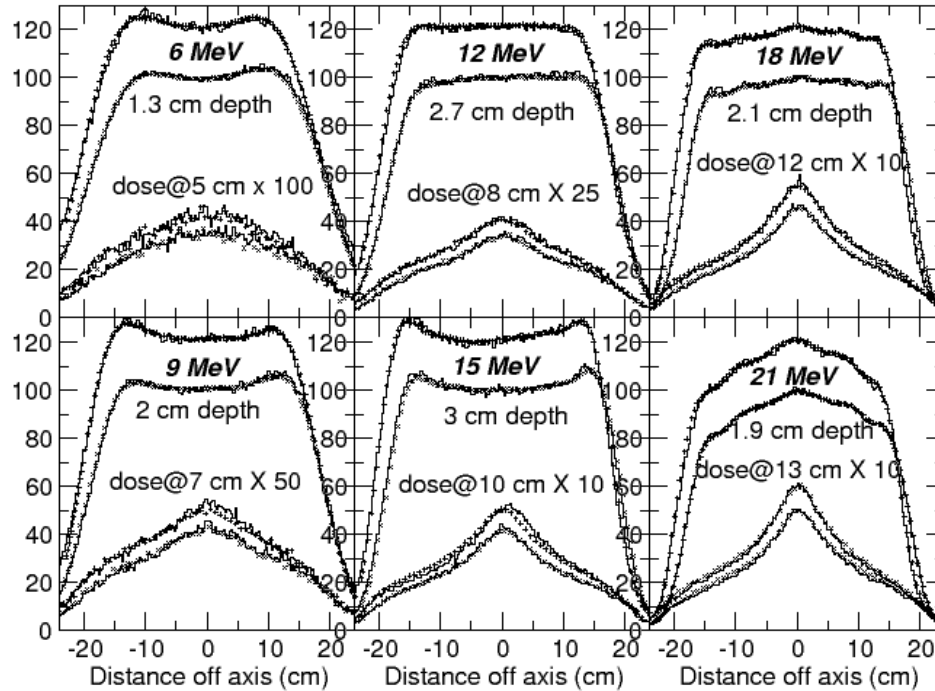


Figure 5. Profiles calculated with EGSnrc (steps) compared to measurements (points). Dose distributions normalized to 100% on the central axis at  $d_{max}$ . The ratio of dose on the central axis at the 2 profile depths was preserved.

correction was applied using commercial software from Wellhofer that is limited to discrete energies.

Differences in the SPR's for mono-energetic and realistic beams do not explain the differences in the measured depth dose curves or differences between the measurements and the Monte Carlo calculations. The depth dose curves in Figures 2 and 3 are normalized to match in the region near  $d_{max}$ . Therefore, the relative change in the correction factor with depth is the important quantity. The relative change in the water-to-air stopping power ratio agrees within 0.5% in the build-up region of the depth-dose curve. There is only a modest change in silicon-to-air SPR in the build-up region (1% or less) and the change is in the direction to increase the discrepancy.

### 3.2 Dose profiles

Measured and calculated profiles are compared in Figures 5 for EGSnrc. Geant4 results calculated with the low-energy physics list are shown in Figure 6. Results are normalized to 100% at  $d_{max}$  on the central axis, with inplane profile doses multiplied by a factor of 1.2 to separate them from the crossplane profiles. The dose at  $R_{p+}$  was multiplied by the factor shown on each plot.

A similar match was achieved for the  $d_{max}$  profiles with measurement with the two codes. Measurement and calculation agree within 2% in the central region of the field out to the point where the dose starts to drop rapidly, near the field edge. The agreement is generally within 3%/3mm outside this region with the exception of the profiles for the 6 MeV beam where a 5% discrepancy is seen. The  $d_{max}$  profiles calculated with Geant4 using the standard physics list matched the measured profiles just as well as those shown in Figure 6 for the low energy physics list.

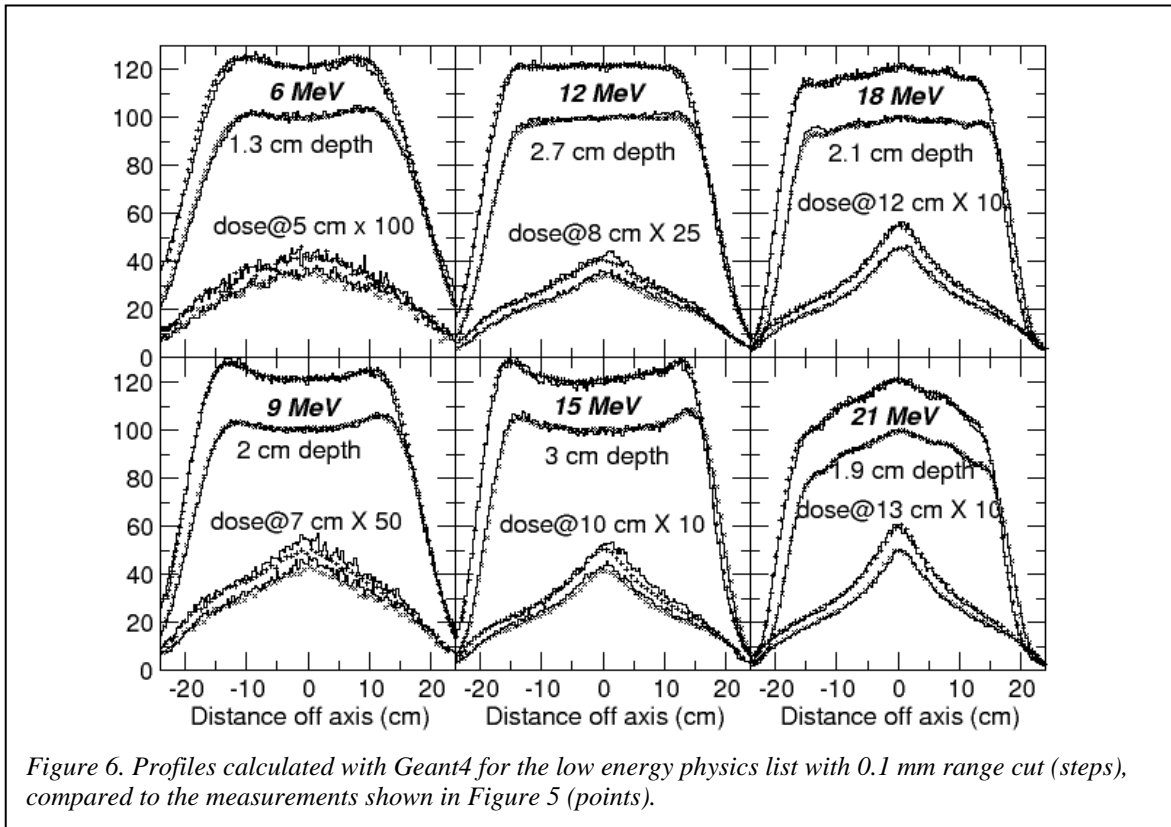


Figure 6. Profiles calculated with Geant4 for the low energy physics list with 0.1 mm range cut (steps), compared to the measurements shown in Figure 5 (points).

Consider the profiles in the bremsstrahlung region, measured just beyond the practical range of each electron beam in the water phantom. EGSnrc and Geant4 with the low energy physics list generally achieved good agreement in the profile shapes and  $D_x/D_e$  with measurement, within experimental uncertainty. The dose in the bremsstrahlung tail was overestimated at 18 and 21 MeV, by 5% and 7%, respectively, when using Geant4 with the standard physics list. Results for 21 MeV are plotted in Figure 7. The overestimate is barely two standard deviations outside the experimental uncertainty and only amounts to a 0.5% dose difference (with dose at  $d_{max}$  normalized to 100%), of little consequence clinically.

The dose in the bremsstrahlung region in the 15 MeV beam was overestimated by 7%, twice the experimental uncertainty, limited to points a few centimeters off axis in the inplane profile, by both EGSnrc and Geant4 with the low energy physics list. The overestimate was 12% with Geant4 when using the standard physics list (profile not shown). Since the dose was overestimated in all cases, the foil may have been too thick in the simulation. It was assumed that the foil thickness would be the same for the 15, 18 and 21 MeV beams, since they share the same foil. However, the inplane steering is different for these beams. It is possible the beam impinges on a different part of the foil at 15 MeV, and the foil thickness may be different at that point.

### 3.3 Simulation parameters

The energy-dependent source and geometry parameters required to obtain a good match with measured data are listed in Table 1. Different parameters were required for the EGSnrc simulations and the Geant4 simulations using the different physics lists. Results in Table 1 show the mean energy of the Parmela spectra, inplane direction cosines of the electron source, and percentage change in the primary scattering foil thickness from the value specified by the manufacturer. The crossplane direction cosine was 0.003 in all cases.

**Table 1.** Energy dependent source and geometry parameters

Monte Carlo System	Mean Energy (MeV)	Inplane Direction Cosine	Foil Thickness Change
EGSnrc	6.82	0.005	0%
Geant4 Standard	6.82	0.003	0%
Geant4 Low energy	6.74	0.005	0%
EGSnrc	9.86	0.003	0%
Geant4 Standard	9.86	0.002	13%
Geant4 Low energy	9.57	0.002	13%
EGSnrc	12.47	0.001	-6%
Geant4 Standard	12.47	0.000	4%
Geant4 Low energy	12.15	0.000	4%
EGSnrc	16.16	0.008	-5%
Geant4 Standard	16.16	0.007	5%
Geant4 Low energy	15.78	0.007	5%
EGSnrc	19.33	0.003	-5%
Geant4 Standard	19.33	0.002	5%
Geant4 Low energy	18.87	0.002	5%
EGSnrc	22.36	0.000	-5%
Geant4 Standard	22.36	-0.001	5%
Geant4 Low energy	21.99	-0.001	5%

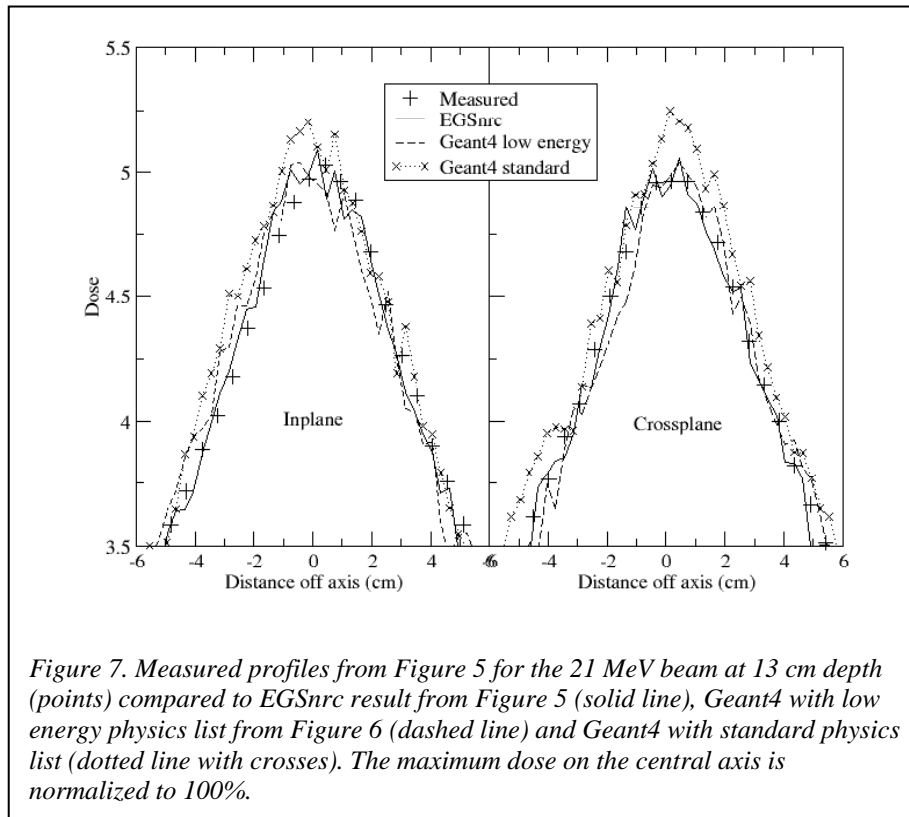
The energy-independent parameters are listed in Table 2. Lateral shifts are relative to collimator rotation axis. Percentage values are the change from the manufacturer specification.

**Table 2.** Energy independent source and geometry parameters.

Parameter	EGSnrc	Geant4 Standard	Geant4 Low energy
Gaussian focal spot FWHM	0.2 cm	0.2 cm	0.2 cm
Exit window thickness	25% thicker	28% thicker	35% thicker
Distance from primary foil to secondary foil	No change	-0.1 cm	-0.1 cm
Secondary foil thickness at center	10% thicker	10% thicker	10% thicker
Foil and foil ring inplane lateral shift	-0.02 cm	-0.02 cm	-0.02 cm
Foil and foil ring crossplane lateral shift	0.006 cm	0.006 cm	0.006 cm
Chamber inplane lateral shift	-0.22 cm	-0.22 cm	-0.22 cm
Chamber crossplane lateral shift	0.016 cm	0.016 cm	0.016 cm

The same mean energy of the electron sources were used for both EGSnrc and Geant4 with the standard physics list. Geant4 with low energy physics required a different mean energy. The maximum difference in mean energy was 0.46 MeV for the 18 MeV beam. According to the sensitivity analysis of Schreiber and Faddegon (2005), this corresponds to a 0.2 cm shift in the depth of the 50% dose on the central axis, a 2% change in the off axis ratio at a point 12 cm off axis and a 2% change in the dose in the bremsstrahlung tail.





The inplane direction cosine was changed by up to 0.002 for simulations of the same beam with the different codes and physics lists. The sensitivity analysis shows this corresponds to a 1-2% change in the off-axis ratio at a point 12 cm off axis.

A thicker exit window and foils are required to match the profiles at  $d_{\max}$  when using Geant4 with either physics list, compared to the EGSnrc simulations. The increased thicknesses correspond to a 2-5% increase in off axis ratio at 12 cm off axis. The foils in the clinical machine used for this study are unavailable for measurement and the exit window is inaccessible. Even if the foils were accessible, the determination of thickness is complicated by the uncertainty of where the beam actually hits the foil, with the foil thickness of the extruded gold foils varying across the foil.

The effect of the different source and geometry parameters on calculated dose distributions, taken individually, is modest at best. As with the foil thickness, the determination of the actual source and geometry parameters to compare to the values used in the simulation is very difficult, especially on a clinical machine where it is highly undesirable to disassemble the treatment head and possibly alter the geometry.

Incorrect values of source or geometry details arise from an insensitivity of the calculated quantity (in this case, dose distributions) to these details or errors in the radiation transport (both the method and the underlying cross-section data). In any case, the accuracy of the fluence may be impacted and may compromise the accuracy of dose calculated in situations very different from the large field: Small fields, fields incorporating surface shielding, treatment of regions with bone, air and other inhomogeneities, irradiation of devices used to measure fluence and dose, etc.

#### 4. Conclusions

Monte Carlo simulation was used successfully to obtain an excellent match to measured large field electron dose distributions. EGSnrc and Geant4 with either physics list are capable of accurate calculation of dose. There was no clear advantage of one code over the other or of one

physics list over the other. Improved agreement may be possible with further adjustment of parameters, including the distance between the different components, the thickness of the scattering foils and the lateral positions of the scattering foil, monitor chamber, and jaws.

Small changes in source and geometry parameters were required for the two codes and two different physics lists to achieve the excellent match obtained between calculated and measured dose distributions. These differences are due to differences in the radiation transport and cross-section data. The differences are within a reasonable tolerance of manufacturer specification. It is not known which parameter set was closest to the actual parameters.

Calculated fluence distributions may not be as accurate as the dose distributions. The small differences in the source and geometry parameters is indicative of small problems with the simulation that could impact on the accuracy of the fluence by 1-2% or so. For one thing, different fluence distributions can result in similar dose distributions. For example, the lower surface dose due to an underestimate of the mean scattering angle of the electron beam incident on a water phantom can be compensated by an overestimate of the number of low energy electrons. For another thing, the details of the radiation transport in the phantom, that is, the conversion from fluence to dose, has a direct impact on the accuracy of the fluence. Thus it is possible to achieve a good match to the measured dose distribution with an incorrect fluence distribution.

A rigorous assessment of the accuracy of the source and geometry parameters and the accuracy of the calculated fluence requires benchmark measurements for electron beams in the radiotherapy energy range scattered from foils of the material and thickness used in radiotherapy. A benchmark set of this sort, with source and geometry details known with greater accuracy than in the clinical situation, is being acquired at the National Research Council of Canada (McDonald et al, 2007).

### **Acknowledgments**

We are grateful for the help Tsakasa Aso and Jane Tinslay gave in writing the code. This work is supported in part by the U.S. Department of Energy under contract number DE-AC02-76SF00515 and the National Institute of Health under R01 CA104777-01A2.

### **References**

Agostinelli S *et al* 2003 Geant4 - A Simulation Toolkit *Nuclear Instruments and Methods in Physics Research A* **506** 250-303

Allison J *et al.* 2006 Geant4 Developments and Applications *IEEE Transactions on Nuclear Science* **53** 270-278

Almond P R, Biggs P J, Coursey B M, Hanson W F, Huq M S, Nath R, and Rogers D W O 1999 AAPM's TG-51 protocol for clinical reference dosimetry of high-energy photon and electron beams *Medical Physics* **26** 1847-1870

Ding D X, Rogers D W O, and Mackie T R 1995 Calculation of stopping-power ratios using realistic clinical electron beams *Medical Physics* **22** 489-501

Faddegon B A, Schreiber E, and Ding X 2005 Monte Carlo simulation of large electron fields *Phys. Med. Biol.* **50** 741-753

Khan F M, Doppke K P, Hogstrom K R, Kutcher G J, Nath R, Prasad S C, Purdy J A, Rozenfeld M, and Werner B L 1991 Clinical electron-beam dosimetry: Report of AAPM Radiation Therapy Committee Task Group No. 25 *Medical Physics* **18** 73-109

Kawrakow I 2000 Accurate condensed history Monte Carlo simulation of electron transport. I. EGSnrc, the new EGS4 version *Medical Physics* **27** 485-98

Rogers D W O, Faddegon B A, Ding G X, Ma C-M, We J, and Mackie T R 1995 BEAM: A Monte Carlo code to simulate radiotherapy treatment units *Medical Physics* **22** 503-524

Ma C-M and Jiang S B 1999 Monte Carlo modelling of electron beams from medical accelerators *Phys. Med. Biol.* **44** R157

McDonald A, McEwen M, Faddegon B, Ross C 2007 High precision data set for benchmarking of electron beam Monte Carlo *Medical Physics* **34** 2457

Poon E and Verhaegen F 2005 Accuracy of the photon and electron physics in GEANT4 for radiotherapy applications *Medical Physics* **32** 1696-711

Schreiber E and Faddegon B A 2005 Sensitivity of large-field electron beams to variations in a Monte Carlo accelerator model *Phys. Med. Biol.* **50** 769-778

Verhaegen F and Seuntjens J 2003 Monte Carlo modelling of external radiotherapy photon beams *Phys. Med. Biol.* **48** R107-R164